Available online at www.sciencedirect.com

ScienceDirect

Geochimica et Cosmochimica Acta 139 (2014) 527–539

Geochimica et Cosmochimica Acta

www.elsevier.com/locate/gca

SIMS measurements of intrashell $\delta^{13}C$ in the cultured planktic foraminifer *Orbulina universa*

Lael Vetter [a,*], Reinhard Kozdon [b], John W. Valley [b], Claudia I. Mora [c], Howard J. Spero [a]

[a] *Department of Earth and Planetary Sciences, University of California Davis, Davis, CA 95616, USA*
[b] *WiscSIMS Laboratory, Department of Geoscience, University of Wisconsin–Madison, Madison, WI 53706, USA*
[c] *Earth and Environmental Sciences Division, Los Alamos National Laboratory, Los Alamos, NM 87545, USA*

Received 12 November 2013; accepted in revised form 30 April 2014; available online 14 May 2014

Abstract

In this study, we present experimental results from the planktic foraminifer *Orbulina universa,* cultured in the laboratory. We demonstrate that the $\delta^{13}C$ of shell calcite precipitated in ^{13}C-labeled seawater for 24 h can be resolved and accurately measured using Secondary Ion Mass Spectrometry (SIMS). Specimens maintained at 20 °C were transferred from ambient seawater ($\delta^{13}C_{DIC} = +1.3‰$) into seawater with $\delta^{13}C_{DIC} = +51.5‰$ and enriched $[Ba^{2+}]$ for 24 h. Specimens were then transferred into ambient seawater with elevated $[^{87}Sr]$ for 6–9 h of calcification, followed by a transfer back into unlabeled ambient seawater until gametogenesis. This technique produced *O. universa* shells with calcite layers of distinct geochemical signatures. We quantify the spatial positions of trace element labels in the shells using laser ablation ICP-MS depth profiling. Using fragments from the same shells, we quantify intrashell $\delta^{13}C_{calcite}$ using SIMS with a 6 or 8 μm spot (2 SD range ±0.5‰ to 1.7‰). Measured $\delta^{13}C_{calcite}$ values in *O. universa* shell layers precipitated in ambient seawater are within 2‰ of predicted $\delta^{13}C_{calcite}$ values. In ^{13}C-labeled bands of calcite, 6 μm SIMS spot measurements are within 2‰ of predicted $\delta^{13}C_{calcite}$ values, whereas 8 μm SIMS spots yield intermediate, mixed values. The spatial agreement between trace element and carbon isotope data suggests that ^{13}C and cation tracers are synchronously incorporated into shell calcite. These results demonstrate the ability of SIMS $\delta^{13}C$ measurements to resolve ~10 μm features in foraminifer shell calcite using a 6 μm spot, and highlight the potential of this technique for addressing questions about ecology, biomineralization, and paleoceanography.

1. INTRODUCTION

Physiological processes such as respiration and symbiont photosynthesis are known to cause variations in the carbon isotopic composition of foraminiferal calcite (Spero et al., 1991). However, the primary parameter controlling the $^{13}C/^{12}C$ ratio in planktic foraminifers is the $\delta^{13}C$ value of dissolved inorganic carbon ($\delta^{13}C_{DIC}$) in seawater (Spero, 1992). As such, foraminifer $\delta^{13}C$ data have been used to reconstruct global carbon cycle dynamics (Zachos et al., 2001, 2005) and ocean circulation (Boyle and Keigwin, 1985; Slowey and Curry, 1995; Billups et al., 2002; Spero and Lea, 2002; Spero et al., 2003) across a range of timescales from Pleistocene glacial-interglacial cycles (Slowey and Curry, 1995) through the Cretaceous (Zachos et al., 2001). All of these studies combined multiple foraminifer shells during a single geochemical measurement, thereby averaging the environmental and/or diagenetic information contained in individual shells. However, each individual foraminifer in a population records seasonal and depth-specific information in its shell chemistry

* Corresponding author. Present address: Department of Earth and Environmental Sciences, Tulane University, New Orleans, LA 70118, USA. Tel.: +1 775 525 0847.
E-mail address: laelvetter@laelvetter.com (L. Vetter).

http://dx.doi.org/10.1016/j.gca.2014.04.049
0016-7037/

(Killingley et al., 1981; Schiffelbein and Hills, 1984), and therefore the bulk analysis approach averages inter-specimen variability and masks the breadth of environmental information potentially available from the fossil record.

Analyses of the intrashell geochemistry in foraminifer shells offer an opportunity to explore short duration events in the life history of a foraminifer. Research on oxygen isotope heterogeneity within foraminifer shell walls using Secondary Ion Mass Spectrometry (SIMS) has been conducted on cultured benthic (Rollion-Bard et al., 2008) and planktic (Vetter et al., 2013a) species, as well as fossil planktic foraminifers (Kozdon et al., 2009, 2011, 2013). Together, these studies have demonstrated that intrashell geochemistry records environmental information with temporal resolution at a finer scale than the lifecycle of foraminifers. SIMS analyses combined with laser ablation inductively coupled plasma mass spectrometry (LA-ICP-MS) depth profiling on cultured specimens of the planktic foraminifer *Orbulina universa* show that oxygen isotope and trace element labeled calcite can be quantified with daily resolution (Vetter et al., 2013a), thereby highlighting the potential for *in situ* multiproxy analyses on foraminifer shells to reconstruct novel paleoenvironmental information from the fossil record.

Although oxygen isotope spot analyses using SIMS have been performed on biogenic carbonates (Rollion-Bard et al., 2003, 2007, 2008; Kozdon et al., 2009, 2011; Allison and Finch, 2010; Hanson et al., 2010; Olson et al., 2012; Matta et al., 2013), the use of SIMS to analyze carbonate $\delta^{13}C$ in foraminifers has not been widely applied. In addition to reconstructing $\delta^{13}C_{DIC}$ in seawater, the carbon isotope composition of foraminifer shells has been used to infer ecological patterns and symbiont activity related to differences in depth habitat within the water column (Williams et al., 1981; Spero et al., 2003), as well as the identification of post-depositional diagenetic carbonate overgrowths that occurred on the seafloor (Lohmann, 1995; Shieh et al., 2002; Millo et al., 2005). Intrashell carbon isotope measurements on fossil foraminifers have the potential to provide insight into these biological, ecological, and diagenetic processes.

The biological and environmental parameters controlling shell $\delta^{13}C$ in the extant planktic foraminifer *O. universa* are well-characterized from laboratory studies, so this species is an ideal organism for investigating intrashell carbon isotope heterogeneity in controlled laboratory experiments (Spero, 1988; Spero and Williams, 1988; Lea and Spero, 1994; Spero et al., 1997; Bemis et al., 2000; Hönisch et al., 2011). *O. universa* produces a single spherical chamber near the end of its life cycle that thickens continuously over the course of 3–7 days (Spero, 1988). Experimental data show that at 20 °C, the $\delta^{13}C$ of shell calcite ($\delta^{13}C_c$) is ~1.2‰ more positive relative to $\delta^{13}C_{DIC}$ when the foraminifer is grown on a 12 h:12 h light:dark cycle under P_{max} light levels during the light phase (Bemis et al., 2000). In contrast, $\delta^{13}C_c$ is similar to $\delta^{13}C_{DIC}$ when *O. universa* is grown continuously in the dark (Spero, 1988). These data allow us to predict the $\delta^{13}C_c$ value of a shell grown in the laboratory in seawater with known $\delta^{13}C_{DIC}$.

In this study, we present the results of laboratory experiments that demonstrate the application of SIMS for intrashell $\delta^{13}C_c$ analyses in *O. universa*. Specimens were maintained in seawater chemically modified through the addition of a ^{13}C-enriched carbon source, as well as elevated $[Ba^{2+}]$ or $[^{87}Sr^{2+}]$ to label calcite with a secondary trace element spike. This technique produced multiple time-resolved bands of calcite with predictable stable isotope and trace element geochemistry (Fig. 1), as described by Vetter et al. (2013a). Specimens were analyzed using SIMS ($\delta^{13}C_c$) and LA-ICP-MS (Ba/Ca and $^{87}Sr/Ca$). Our results suggest that it is possible to use spot $\delta^{13}C_c$ analyses on fossil shells to explore ecological aspects of foraminifer lifecycles in ~10 μm wide features in calcite, which corresponds to 2–3 day resolution (Spero, pers. comm).

2. METHODS

2.1. Culturing experiments

Individual *O. universa* specimens were cultured using previously established procedures (Bemis et al., 1998; Russell et al., 2004; Vetter et al., 2013a) at the Wrigley Marine Science Center, Santa Catalina Island, California, USA. Juvenile, trochospiral *O. universa* were hand-collected by scuba divers in the San Pedro Basin in the Southern California Bight (33°23′N, 118°26′W) at a depth of 2–5 m. Individual *O. universa* were grown in the laboratory at a constant temperature of 20 °C on a 12 h:12 h day:night light cycle under "high-light" (HL) conditions (>386 μmol photons m^{-2} s^{-1}, PAR; Bemis et al., 2000). Each foraminifer was fed one 1-day-old *Artemia* nauplius every other day. Juvenile, trochospiral specimens were maintained in ambient seawater filtered through 0.8 μm nitrate cellulose filters until they precipitated their final spherical shells. As a control for the experiment, one set of individual *O. universa* was cultured in ambient seawater until gametogenesis (Table 1). These shells were predicted to have intrashell geochemistry that reflects a stable chemical environment.

A second group of foraminifers was used for a series of geochemical labeling experiments in seawater with modified trace element and stable isotope chemistry (Vetter et al., 2013a). Experimental seawater was labeled with elevated Ba via the addition of concentrated $BaCl_2$ spike solution ($[Ba] = 720$ μmol kg^{-1}). The calculated final $[Ba/Ca]_{sw} =$ 39 μmol mol^{-1} (~4× ambient), although some of the excess Ba may have been scavenged by precipitation of barite. This Ba-labeled seawater was also modified by the addition of 99.1% $Na_2{}^{13}CO_3$ to produce seawater with a $\delta^{13}C_{DIC}$ (~+50‰). Following the addition of the ^{13}C label, HCl was then added to the experimental seawater to return the alkalinity to ambient levels (~2250 μmol kg^{-1}). After preparation of the ^{13}C label, double-labeled seawater was maintained with no head space in 20 ml scintillation vials sealed with Parafilm® and plastic polyseal caps, to minimize isotopic exchange with atmospheric CO_2. The duration of exposure to atmosphere during foraminifer transfers was also minimized. A second batch of labeled seawater was prepared with ^{87}Sr ~2.5× ambient $[^{87}Sr]$ in seawater, via the addition of concentrated $^{87}SrCO_3$ in solution (calculated final $[^{87}Sr] = 14.0$ μmol kg^{-1}) to use as a trace-element-only label.

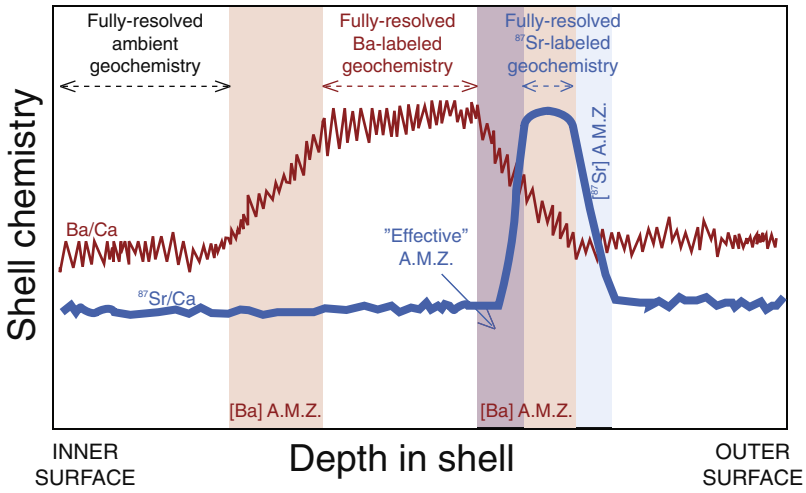

Fig. 1. Idealized LA-ICP-MS depth profile showing shell chemistry changes in a foraminifer shell wall as Ba (red) and ^{87}Sr (blue) concentrations in seawater are shifted between ambient and Ba or ^{87}Sr-labeled seawater. Some labeled or ambient regions of the shell are sufficiently thick to fully resolve the trace element signal, whereas mixing occurs in zones that are thinner than the sample spot diameter or resolution of the laser ablation technique (analytical mixing zone; AMZ); the latter scenario yields intermediate values. The instantaneous transfer from Ba-labeled seawater into ^{87}Sr-labeled seawater is represented by two contemporaneous, overlapping AMZs, as Ba/Ca ratios decrease and ^{87}Sr/Ca ratios increase. The geochemical transition between the two trace element labels in shell calcite is defined where Ba/Ca begins to decrease and where ^{87}Sr/Ca ratios fully resolve labeled geochemistry.

All geochemical labeling experiments were conducted during the sphere-thickening phase of chamber growth and at a constant temperature of 20 °C. Although *O. universa* secretes 66% of its shell during daylight hours, some evidence suggests that calcification rates peak at ~13:00 (6 h after the start of the day cycle; Spero and Parker, 1985; Lea et al., 1995). To investigate the incorporation of a ^{13}C-enriched tracer during calcification, we performed two complementary labeling experiments with different timing with respect to the day/night cycle. Individual adult *O. universa* were transferred via pipette into seawater that was enriched in both Ba and ^{13}C at the start of a 12 h light period (07:00) and maintained at 20 °C (Fig. 2). These individuals were maintained in labeled solution through a full 12 h light and 12 h dark period ("synchronous" labeling experiment), and then transferred into ^{87}Sr-labeled seawater at the start of the subsequent 12 h light period (07:00 the following day; Table 1). Individuals were then transferred back into ambient seawater after 6 h of calcification in ^{87}Sr-labeled seawater, and maintained in ambient seawater until gametogenesis.

The two consecutive trace element labels mark the location within shell calcite of the transition between ^{13}C-labeled seawater (Ba-labeled) and ambient seawater (^{87}Sr-labeled). The spatial resolution with which this dual transition in trace element labels can be measured is thus higher than the spatial resolution achievable via *in situ* δ^{13}C analyses. In a parallel experiment, we followed the same procedure but offset the transfers from the initiation of a light/dark cycle by 6 h ("offset" labeling experiment; Fig. 2). Individual foraminifers were transferred into Ba- and ^{13}C-labeled calcite midway through a light cycle (13:00), and then maintained in this spiked solution for the next 24 h. Midway through the next light cycle (13:00 the following day), individuals were transferred into ^{87}Sr-labeled seawater, calcified for 9 h (6 h in the light, 3 h in the dark), after which the specimens were transferred back into ambient seawater and maintained until gametogenesis (Table 1).

Table 1
Summary of cultured *O. universa* specimens, showing experimental regime, synchroneity of ^{13}C-labeled incubation with day/night cycle, and duration of calcification in each labeled seawater.

Specimen number	Ambient or labeled	Day/night cycle	Time duration in Ba- and ^{13}C-labeled seawater (h)	Time duration in ^{87}Sr-labeled seawater (h)
SV-50	Ambient	–	–	–
SV-37	Label	Synchronous	24	6
SV-41	Label	Synchronous	24	6
SV-45	Label	6 h offset	24	9
SV-51*	Label	6 h offset	24	9

* Specimen was analyzed via SIMS using both 6 and 8 μm spot sizes.

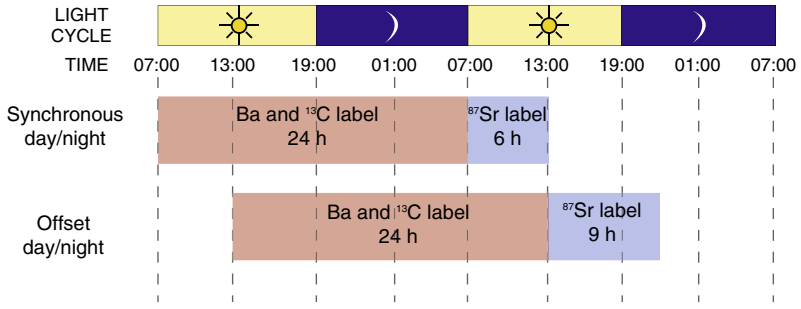

Fig. 2. Schematic diagram of two sets of labeling experiments: [Top] For *O. universa* specimens with ^{13}C label synchronous with day/night cycle, individuals calcified in Ba- and ^{13}C-labeled seawater for 24 h (07:00 to 07:00), then were transferred to ^{87}Sr-labeled seawater for 6 h of calcification. [Bottom] For *O. universa* specimens with ^{13}C label offset from day/night cycle, individuals calcified in Ba- and ^{13}C-labeled seawater for 24 h (13:00 to 13:00), then transferred to ^{87}Sr-labeled seawater for 9 h. See Section 2.1 for detailed culture methods. These two sets of geochemical labeling experiments are referred to as "synchronous" and "offset", respectively.

To minimize contamination between labeled solutions, individual *O. universa* were pipetted through two intermediate transfer solutions that contained the same seawater (labeled or ambient) as the destination jar, and then into the destination solution for the calcification interval. After incubation in ^{87}Sr-labeled seawater, each specimen was maintained in filtered seawater at 20 °C until gametogenesis.

Following gametogenesis, the empty shells were rinsed in deionized water and archived individually for later analysis. Prior to trace element and $\delta^{13}C$ analyses, individual *O. universa* shells were manually cracked into several fragments using a disposable scalpel, and isolated and cleaned for 10 min in a 1:1 solution of 30% H_2O_2 and 0.1 N NaOH at 65 °C to remove residual organic matter. Shell fragments were then rinsed in deionized water, sonicated for 10–15 s in reagent grade methanol to remove any remaining adherent material, and rinsed two additional times in deionized water.

Water samples were collected prior to the initiation of an experiment for analysis of $\delta^{13}C_{DIC}$. Samples were poisoned with 1–2 drops (~0.5 ml) of a saturated $HgCl_2$ solution and stored in vials without headspace. Vials were sealed with cap and cone seals, and a double layer of Parafilm®, until analysis. Culture water $\delta^{13}C_{DIC}$ was determined by injecting 5 ml of seawater into 105% orthophosphoric acid under vacuum. Acid-stripped CO_2 was cryogenically purified and collected in 6 mm Pyrex tubes. The $\delta^{13}C$ values of extracted CO_2 were measured on a Fisons Optima gas source isotope ratio mass spectrometer (IRMS), with analytical precision of $\pm 0.03‰$ relative to VPDB.

2.2. Laser ablation ICP-MS analyses

For this study, we analyzed one specimen cultured continuously in ambient seawater, two specimens from the "light-synchronized" experiment, and two specimens from the "offset" experiment. One fragment of each shell was analyzed for trace element ratios using laser ablation inductively coupled plasma mass spectrometry (LA-ICP-MS). Trace element concentrations were measured using a 193 nm Photon Machines ArF Excimer laser with dual-volume cell, coupled to an Agilent 7700x quadrupole ICP-MS, in the Stable Isotope Laboratory, Department of Earth and Planetary Sciences, at the University of California, Davis. The fragments were mounted on double-sided adhesive carbon tape, oriented with the shell interior facing upwards, and ablated in depth profile at 5 Hz using a laser fluence of 1.46 J cm^{-2} and a 30 μm diameter spot. The Helex dual volume sample chamber exhibits 99% washout within 2 s ($t_{1/2} = 0.75$ s), so samples can be ablated in depth profile rapidly. The operating conditions of the LA-ICP-MS

Table 2
LA-ICP-MS system operating conditions.

ICP-MS: Agilent 7700x	
RF power	1500 W
Argon gas flow	1.05 L min^{-1}
Coolant gas flow	15 L min^{-1}
Auxiliary gas flow	1 L min^{-1}
Dwell time per mass	20–100 ms
Monitored masses (m/z)	^{24}Mg, ^{25}Mg, ^{27}Al, ^{43}Ca, ^{44}Ca, ^{55}Mn, ^{87}Sr, ^{88}Sr, ^{138}Ba
Laser ablation system: Photon Machines 193 nm ArF Excimer	
Energy density (fluence)	1.5–3.1 J cm^{-2}
He gas flow	1.05 L min^{-1}
Laser repetition rate	5 Hz
Laser spot size	30 μm
ThO^+/Th^+	<0.5%

system during data collection are summarized in Table 2. Previous studies have demonstrated that an ablation pit with a high aspect ratio (depth/diameter > 2) can cause elemental fractionation that will affect measured isotopic ratios (Eggins et al., 1998; Mank and Mason, 1999; Woodhead et al., 2004). However, with an average *O. universa* shell thickness of 20–25 μm and ablation spot of 30 μm, the aspect ratio in our specimens is <1, and elemental fractionation with increasing pit depth is not a factor.

Two or three replicate depth profiles were ablated on each shell fragment. Samples were analyzed for ^{24}Mg, ^{25}Mg, ^{27}Al, ^{43}Ca, ^{44}Ca, ^{55}Mn, ^{87}Sr, ^{88}Sr, and ^{138}Ba, with a mean dwell time of 0.030 s on each mass. Raw data for depth profiles were smoothed using two separate despiking routines to remove anomalously high outliers: first an exponential decay smoothing, then removing values that are >6 SD greater than the two adjacent points. From the smoothed signal, we then subtracted background counts, measured with the laser turned off, and internally standardized to ^{43}Ca and ^{44}Ca. An initial pulse of high count rates in all the elements we measured comprises an instrumental effect from transport of the sample from laser to plasma, and was thus removed from the depth profile (Vetter et al., 2013b). This signal is separate from the biogenic signal of high Ba/Ca and ^{87}Sr/Ca that remains in each depth profile, which represents calcite with a trace element label that was precipitated inside of the primary organic membrane (Sadekov et al., 2010).

Using this approach, the typical external (spot-to-spot) precision on unlabeled specimens is 0.004 μmol mol^{-1} for Ba/Ca and 0.2 μmol mol^{-1} for ^{87}Sr/Ca (2 SD). The intensity of the ^{27}Al signal was monitored to identify phases of the depth profile where portions of the carbon tape influence time-resolved analyses and may compromise computed elemental ratios. An identical ablation protocol was performed on a NIST 610 glass standard to bracket each group of 10–15 samples, at a higher fluence (3.1 J cm^{-2}; Table 2) so that trace elemental count rates from the NIST 610 glass were approximately the same as foraminiferal calcite ablated at lower fluence. Elemental ratios for shell material were quantified by correcting measured intensities on shell material to measured elemental intensities on the NIST 610 glass in the same sample bracket, and internally standardized to ^{43}Ca and ^{44}Ca (Eggins et al., 2003, 2004; Bolton et al., 2011; Jonkers et al., 2012; Marr et al., 2013).

2.3. *In situ* δ^{13}C analyses using SIMS

The LA-ICP-MS depth profiles of intrashell Ba and ^{87}Sr on one fragment of each individual delineate the position within the shell when the foraminifer was transferred into ^{13}C-labeled seawater, and from ^{13}C-labeled seawater into the secondary labeled seawater solution (Fig. 2). A second fragment of each shell was mounted together with 2–3 grains of UWC-3, the WiscSIMS calcite standard ($\delta^{13}C = -0.91 \pm 0.04‰$ VPDB, $\delta^{18}O = +12.49 \pm 0.03‰$ VSMOW; Kozdon et al., 2009) in Buehler EpoxiCure resin in a 25 mm epoxy round. These epoxy rounds were ground to 20–40 μm depth to expose oblique cross-sections of shell walls, which increases the surface area and spatial resolution able to be achieved through consecutive spot analyses. Samples were then polished, and finally cleaned with ethanol and deionized water while minimizing exposure time to prevent etching. Subsequently, sample mounts were gold-coated. Scanning electron microscope (SEM) images of the polished, gold-coated samples were used to gauge calcite porosity in mounted shell material and to screen samples for textural anomalies that might compromise *in situ* δ^{13}C measurements.

Cultured foraminifer shells were analyzed for δ^{13}C on a CAMECA ims-1280 secondary ion mass spectrometer (SIMS) using a $^{133}Cs^+$ primary ion beam at the WiscSIMS Laboratory, Department of Geoscience, University of Wisconsin-Madison. For the majority of the analyses, a primary beam of 600 pA was used with an 8 μm spot size. A second set of measurements was performed on one sample (SV-51, fragment C) with a 250 pA primary beam and 6 μm spot size, to increase the spatial resolution of measurements. The secondary ^{12}C and ^{13}C ions were simultaneously collected on a Faraday cup and electron multiplier, respectively. Secondary count rates on ^{12}C were ~5×10^6 cps for the 600 pA beam and ~1.5×10^6 cps for the 250 pA beam. The resistance on the Faraday cup was $10^{11}\Omega$, with background variation ("noise") of ±1000 cps on ^{12}C (±1 SD). Each analysis comprises 20 s of presputtering, automatic centering of the secondary ions in the field aperture (~60 s), and 20 analytical cycles of 8 s each.

Analyses of sample material (10–12 spot analyses per group) were bracketed by 8–12 repeat measurements on the UWC-3 standard grain, using analytical conditions identical to those used during sample analysis. The gain of the electron multiplier was monitored before the third analysis of each group of calcite standard measurements, and the applied high voltage was adjusted to compensate for the drift of the gain of the electron multiplier, if necessary. The bracketing analyses of the UWC-3 standard grain were used to determine instrumental mass fractionation corrections for each set of measurements on foraminiferal calcite. The external precision reported for sample measurements is the spot-to-spot reproducibility of the 8–12 repeat measurements on the UWC-3 standard grain that bracket each set of sample analyses, and ranges from ±0.5‰ to 1.8‰ (2 SD; Table S1). Analytical pits that extended into epoxy and/or organic material can be recognized by anomalously high secondary count rates (>100% of the measured counts per second on the standard grain). For 5 of 116 measurements, the SIMS analysis pit expanded into these domains during the later analytical cycles (out of 20 total), compromising data quality. For measurements in which this occurred, the final ~5 cycles that showed an increased count rate were excluded from computations, and the δ^{13}C value for the spot was recalculated based on cycles 1–15. Data processed using this approach are indicated in Table S1 with the symbol †. The complete dataset, including measurements on standard grains, is available in the Electronic Annex.

On each cultured foraminifer shell, we performed a suite of spot measurements across the direction of shell wall thickening. Individual measurements were placed in calcite domains within the shell that were preselected by observation

of SEM images to avoid cracks, epoxy, cross-sectional exposures of pore spaces within the shell, and areas of the shell with organic matter not removed by the post-mortem H_2O_2 cleaning process. After performing $\delta^{13}C$ SIMS analyses, a second SEM image was collected of analysis pits, to assess textural features that might have affected the accuracy of spot analyses. Using these post-analysis SEM images, the distance from the interior growth surface of the shell to each pit was measured, and is reported in Table S1.

3. RESULTS

Specimen SV-50 was cultured continuously in ambient seawater during calcification of the final spherical chamber, with constant Ba/Ca, $^{87}Sr/Ca$, and $\delta^{13}C_{DIC}$ (predicted ambient value = +2.5‰; Table 1). The mean whole-shell Ba/Ca ratio for this specimen, averaged from 3 depth profiles ablated through the entire shell, is 0.5 μmol mol^{-1}, with external spot-to-spot reproducibility of 0.002 μmol mol^{-1} (2 SD; Fig. 3a). This ratio is similar to measured Ba/Ca in *O. universa* cultured under similar conditions in ambient seawater (Ba/Ca_{shell} = 0.6–0.7 μmol mol^{-1}; Hönisch et al., 2011); measured $[Ba]_{sw}$ = 36–38 nmol kg^{-1} in the North Pacific (Bernat et al., 1972; Hönisch et al., 2011). The mean whole-shell $^{87}Sr/Ca$ is 319 μmol mol^{-1}, with external spot-to-spot reproducibility of 0.1 μmol mol^{-1} (2 SD). A similar empirical calibration has not been performed for Sr/Ca in *O. universa*, so we use measured intrashell $^{87}Sr/Ca$ as a qualitative label to resolve the transition between calcite precipitated in ^{13}C-labeled and ambient seawater.

Measured $\delta^{13}C_{DIC}$ values for water samples are reported in Table 3. The mean $\delta^{13}C_{DIC}$ value for ambient water or seawater with the ^{87}Sr label is +1.3 ± 0.1‰ (±2 SE, n = 5; Table 3). The initial preparation of ^{13}C-labeled seawater had $\delta^{13}C_{DIC}$ = +53.15‰ VPDB, whereas two water samples collected at the conclusion of the culturing experiments had $\delta^{13}C_{DIC}$ values of +50.58‰ and +50.72‰, respectively. The decrease in $\delta^{13}C_{DIC}$ between experiment initiation and end is likely due to a small amount of CO_2 equilibration with the atmosphere during feeding and transfer sessions. This $\delta^{13}C$ decrease across our labeled experiments adds an uncertainty of ~2.5‰ to the expected shell $\delta^{13}C$ values that are based on average culture data from ambient *O. universa* $\delta^{13}C$ experiments (Bemis et al., 2000) and the assumption that $\delta^{13}C_c$ shifts 1:1 with $\delta^{13}C_{DIC}$ (Spero, 1992). Interestingly, we do not observe a similar decrease in $\delta^{13}C_{DIC}$ in the ambient seawater experiments. We attribute this difference to the fact that the isotopic fractionation between the atmosphere ($\delta^{13}C_{atm} \sim -8$‰; CDIAC, 2014) and seawater at 20 °C is ~8.5‰ (Zhang et al., 1995). Hence, atmospheric CO_2 has little effect on seawater $\delta^{13}C_{DIC}$ of 1.3‰, but a very large effect when $\delta^{13}C_{DIC}$ = +50‰.

Multiple intrashell SIMS analyses were conducted with an 8 μm spot size on two separate fragments (B and C) from specimen SV-50 (Fig. 3b). These analyses yield mean $\delta^{13}C_c$ values of +3.6 ± 0.2‰ (±2 SE, n = 16, fragment B) and +4.5 ± 0.6‰ (±2 SE, n = 8, fragment C). These values are 1–2‰ higher than we would predict from whole shell analyses of ambient specimens ($\delta^{13}C$ = 2.5‰) based on group mean results for *O. universa* grown under similar light:dark conditions at 22 °C (Bemis et al., 2000). However, we note that individual shells display a range of values and our data are close to one of the values, 3.5‰, obtained from an individual in those experiments.

Fig. 4 shows 8 μm spot size data from two *O. universa* specimens (SV-37 and SV-41) from the "light-synchronized" labeling experiment, that began at the start of a 12 h light period (@07:00) and calcified in labeled seawater for 24 h. The initial rise and plateau of shell Ba/Ca delineates the spatial position of calcite precipitated in Ba- and ^{13}C-labeled seawater. The position where the shell records decreasing Ba/Ca and rising $^{87}Sr/Ca$ identifies the start of calcite precipitating in the ^{87}Sr-labeled seawater. The analytical mixing zones delineated by rising and falling Ba/Ca ratios indicate that these laser ablation conditions require 4–10 s of ablation time to fully resolve a band of ambient or labeled shell chemistry calcified over 24 h (Fig. 4a and d). In specimen SV-37 (Fig. 4), all of the $\delta^{13}C_c$ spot measurements within the ^{13}C-labeled calcite band yield values that are intermediate between those predicted for ambient and labeled calcite, ranging from 22.9‰ to 33.6‰ (VPDB; Table S1). In the ambient calcite bands, 7 of 11 spots also yield intermediate values (11.7–34.4‰), whereas the remaining 4 spots yield mean $\delta^{13}C_c$ values of +2.1 ± 3.1‰ (2 SE, n = 4; Table S1) that are close to predicted values. In specimen SV-41 (Fig. 4), all of the $\delta^{13}C_c$ spot measurements within ^{13}C-labeled calcite bands yield intermediate values (33.8–36.2‰; Table S1) whereas only 3 of 11 spot measurements in ambient bands yield intermediate $\delta^{13}C_c$ values (24.9–38.8‰). The remaining 8 spot analyses in ambient calcite have a mean $\delta^{13}C_c$ = +4.6 ± 1.0‰ VPDB (2 SE, n = 8), which is consistent with measured values on ambient calcite in the control specimen (Fig. 3).

Intrashell Ba/Ca, $^{87}Sr/Ca$, and $\delta^{13}C_c$ for two "offset"-labeled *O. universa* specimens, in which shell Ba and ^{13}C labeling was initiated 6 h into the light/dark cycle and continued for 24 h (13:00–13:00 h), are presented in Figs. 5 and 6. Nine hours of ^{87}Sr-labeled calcite (ambient $\delta^{13}C_{DIC}$) followed this treatment. For specimen SV-45, which was analyzed with an 8 μm spot size (Fig. 5), we again observe intermediate values for all of the SIMS measurements within the ^{13}C-labeled calcite band, ranging from 20.6‰ to 36.0‰ (Fig. 5b). In this specimen, we obtained measurements on ambient calcite precipitated prior to the labeling experiment (closer to the inner shell surface) because this foraminifer had added sufficient calcite to permit SIMS analyses on the earliest calcite laid down during sphere formation (Figs. 5b and 6b). In this region of the shell, which was precipitated in ambient seawater, 2 of 13 spot measurements are within 1.7‰ (the most conservative precision achieved for any single bracket in our analytical session) of the predicted ambient value, and 11 pits record intermediate values that range from 7.9‰ to 32.3‰ (Table S1).

Fig. 6b shows $\delta^{13}C_c$ data for two separate fragments of specimen SV-51: closed symbols are 8 μm spot analyses, and open circles are analyses performed using a lower primary beam intensity and a 6 μm spot size. Within the 6 μm spot analyses in the band of Ba- and ^{13}C-labeled

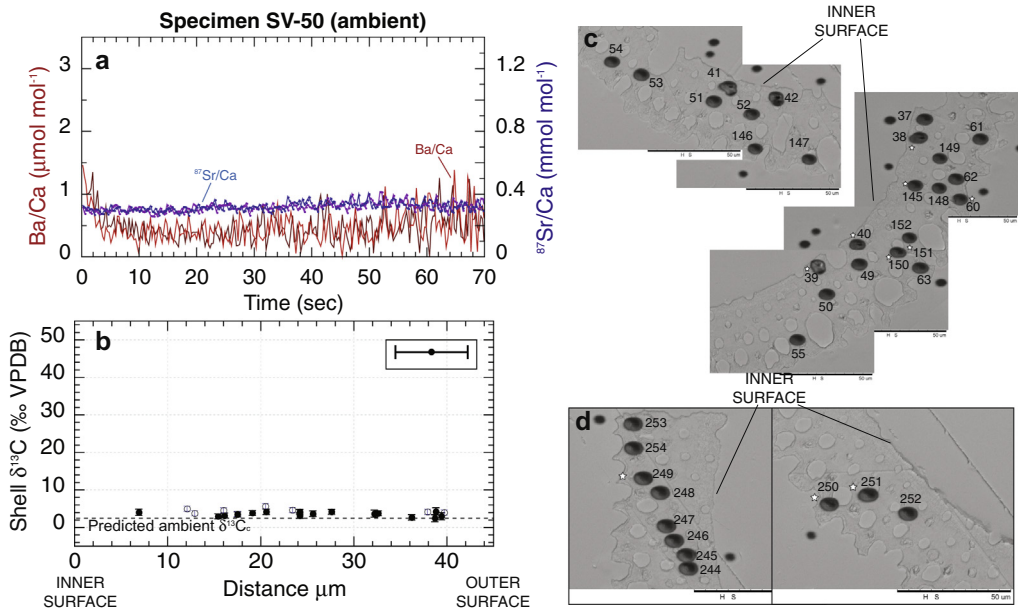

Fig. 3. Measured intrashell Ba/Ca (red) and $^{87}Sr/Ca$ (blue) from 3 or 4 repeat LA-ICP-MS depth profiles (a) and $\delta^{13}C_c$ from SIMS measurements (b) for a single *O. universa* (SV-50) cultured continuously in ambient seawater with constant Ba/Ca, $^{87}Sr/Ca$ and $\delta^{13}C_{DIC}$. Panels (c) and (d) show SEM images of *O. universa* shell walls and the position of SIMS analysis pits for the two separately mounted fragments: pit numbers refer to spot analyses reported in Table S1, and pits marked with a star were excluded due to high count rates. Intrashell $\delta^{13}C_c$ measurements in (b) are from transects across two different fragments of the same shell (closed and open symbols). Horizontal dashed lines show predicted value for $\delta^{13}C_c$ using empirical calibrations for *O. universa* (Bemis et al., 2000). Box in (b) shows horizontal spatial range of 8 μm analysis spots; analytical precision (vertical error bars) are shown on spots where ±2 SD is larger than the size of the symbol.

seawater, 8 of 17 pits yield fully-resolved ^{13}C-labeled values that range between 50.2‰ and 54.6‰ (Table S1). These data agree well with the predicted $\delta^{13}C_c$ values of +51.8‰ to +54.4‰, which are based on the *O. universa* biological offset of 1.3‰ more positive from the initial and final seawater $\delta^{13}C_{DIC}$ water measurements (Table 3). In contrast, none of the 8 μm spot analyses yield full labeled $\delta^{13}C_c$ values (Table S1). Among the spot analyses in the ambient calcite section of the shell, 7 of 22 spots yield values within 1.7‰ of the predicted ambient value of 2.5‰, and 15 values are intermediate (ranging from 5.0‰ to 20.9‰).

4. DISCUSSION

4.1. Intrashell $\delta^{13}C$ measurements using SIMS

Previous SIMS studies on planktic foraminifers have employed 2 to 6 μm beam diameters to measure intrashell $\delta^{18}O_c$ (Kozdon et al., 2009; Vetter et al., 2013a). Vetter et al. (2013a) demonstrated that a 3 μm Cs^+ beam diameter could resolve 18‰ shifts in *O. universa* shell $\delta^{18}O$ that were laid down in laboratory experiments during 12 h periods of calcification (2–3 μm wide calcite bands). In these studies, specimens were mounted with shell cross-sections orthogo-

Table 3
Measured $\delta^{13}C_{DIC}$ of water samples and predicted *O. universa* $\delta^{13}C_c$.

Sample type	Sample number	Measured $\delta^{13}C_{DIC}$ (‰ VPDB)	Mean (‰ VPDB)	Precision (±2 S.E.)	Predicted* shell $\delta^{13}C_c$ (‰VPDB)
Ambient	11-C6-A	1.37			
Ambient	†11-C5-Sr-1	1.45			
Ambient	11-C9-A	1.06	1.27	0.14	2.48
Ambient	†11-C5-Sr-2	1.32			
Ambient	11-C3-A	1.16			
^{13}C-label	‡11-C1-B4I-1	53.15	–	–	54.36
^{13}C-label	‡11-C11-B4F-2	50.58	–	–	51.79
^{13}C-label	‡11-C12-B4F-1	50.72	–	–	51.93

* Predicted $\delta^{13}C_{DIC}$ calculated using the high light (HL) relationship of Bemis et al. (2000) for *O. universa* calcifying at 20 °C.
† Denotes samples of seawater with ^{87}Sr label and ambient $\delta^{13}C_{DIC}$.
‡ Denotes samples of seawater with Ba and ^{13}C labels.

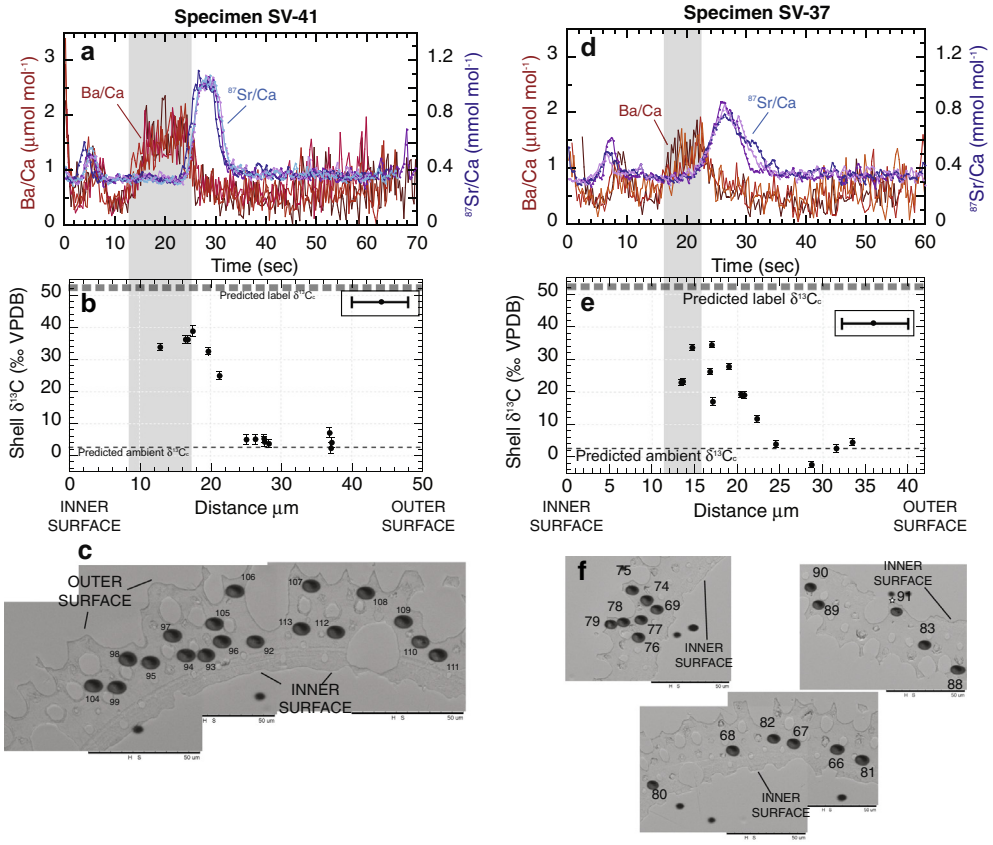

Fig. 4. Ba/Ca (red) and $^{87}Sr/Ca$ (blue) LA-ICP-MS depth profiles (a and d), intrashell $\delta^{13}C_c$ (b and e), and corresponding SEM images of SIMS analysis pits (c) for two *O. universa* specimens (SV-41: a–c; SV-37: d–f) cultured in a 24 h labeling experiment synchronous with the 12 h light/dark cycle; pit numbers refer to spot analyses reported in Table S1. Horizontal dashed lines show predicted $\delta^{13}C_c$ using empirical calibrations for *O. universa* (Bemis et al., 2000). Boxes in (b) and (e) show horizontal spatial range of 8 μm analysis spots; analytical precision (vertical error bars) are shown on spots where ±2 SD is larger than the size of the symbol. The shaded box denotes calcification period in Ba- and ^{13}C-labeled seawater, and is bounded by the analytical mixing zone between labeled and ambient calcite.

nal to the Cs^+ beam. Because $\delta^{18}O_c$ in foraminifer shells is controlled by $\delta^{18}O_{seawater}$ and a temperature-dependent equilibrium fractionation between calcite and water, and $\delta^{13}C$ tracks $\delta^{13}C_{DIC}$, one should be able to resolve ^{13}C and ^{18}O labels in a shell with similar resolution. Unfortunately, carbon has a lower ionization efficiency (Wilson, 1995) and lower concentration in $CaCO_3$ than oxygen, so carbon isotope measurements in $CaCO_3$ require a larger spot size, associated with a stronger beam, to achieve comparable precision (<1‰). The selected primary beam intensity and analysis time for $\delta^{13}C$ analyses was optimized for high analytical precision and accuracy. Besides counting statistics, factors such as the drift of the gain of the electron multiplier and changing sputtering characteristics with increasing pit depths need to be considered (Valley and Kita, 2009). Typically, the 8 μm beam provides the best results for $\delta^{13}C$; however, in this session, the analytical precision was comparable with the smaller (6 μm) beam.

The $\delta^{13}C_c$ measurements we present here were performed on polished oblique cross-sections, so the spatial resolution of exposed shell layers is maximized (Fig. 7a) to try to capture 24 h of calcite (3–4 μm wide band) with a wider diameter spot size of 6–8 μm × ~1 μm deep. Intrashell $\delta^{13}C$ values measured with an 8 μm spot fall between predicted values for calcification in ambient or labeled seawater. Using this spot diameter, the maximum $\delta^{13}C$ values we obtain are +38.8 ± 1.6‰ (2 SD) in specimen SV-41 (Fig. 4), 34.4 ± 1.0‰ (2 SD) in specimen SV-37 (Fig. 4), 36.0 ± 0.7‰ (2 SD) in specimen SV-45 (Fig. 5), and +48.4 ± 1.4‰ (2 SD) in specimen SV-51 (Fig. 6). These values all suggest a mixture of calcite between ambient (+2.5‰) and labeled (+55‰) $\delta^{13}C$ values. In one of these specimens (SV-51), we reduced the SIMS spot size to 6 μm and performed a second transect of measurements (Fig. 6b, fragment C, open symbols), and obtained three values that averaged 54.3‰ (100% labeled calcite), given the precision of these measurements (+1.3‰ (2 SD)). The LA-ICP-MS data for $^{87}Sr/Ca$ and Ba/Ca were generated by ablating a shell surface orthogonal to the laser beam, so the widths of bands with trace element labels cannot be directly compared to the shell thickness of the obliquely polished cross-section measured via SEM. Instead, we conduct a simple mass balance calculation, assuming the maximum value obtained with the 8 μm beam in specimen

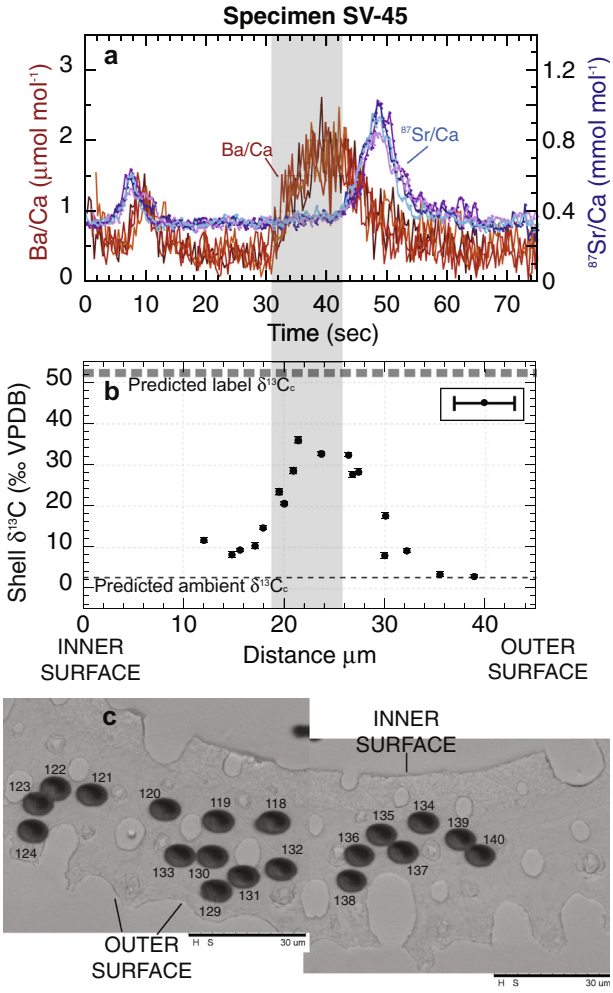

Fig. 5. Ba/Ca (red) and $^{87}Sr/Ca$ (blue) depth profiles (a), intrashell $\delta^{13}C_c$ (b), and corresponding SEM images of SIMS analysis pits (c) for an *O. universa* specimen (SV-45) cultured in a 24 h labeling experiment offset 6 h from light/dark cycle. See caption for Fig. 4 for detailed figure explanation.

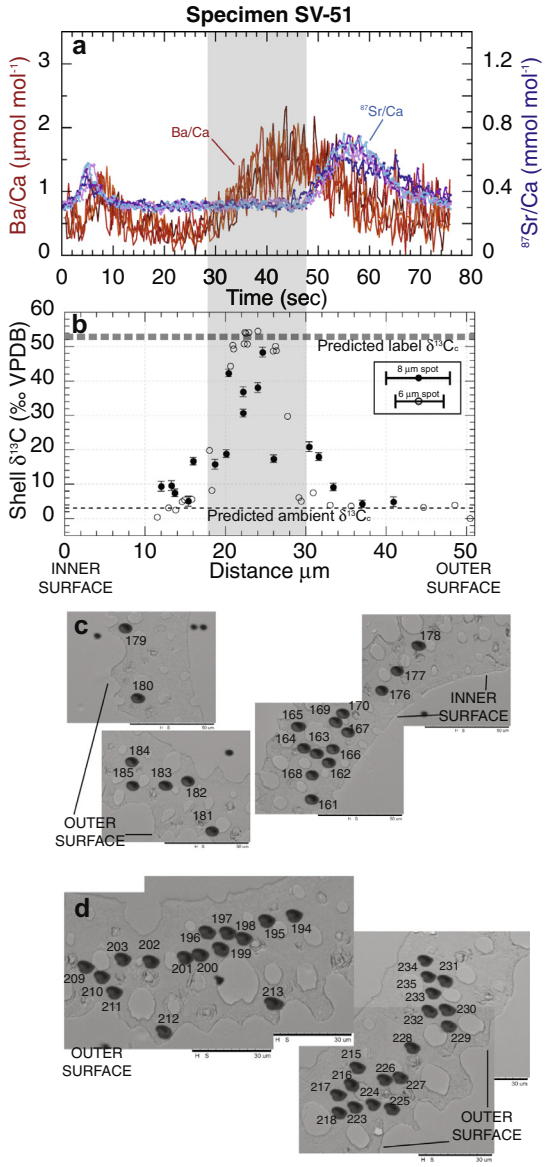

Fig. 6. Ba/Ca (red) and $^{87}Sr/Ca$ (blue) depth profiles (a), intrashell $\delta^{13}C_c$ (b), and corresponding SEM images of SIMS analysis pits (c) for an *O. universa* specimen (SV-51) cultured in 24 h labeling experiments offset 6 h from light/dark cycle; pit numbers refer to spot analyses reported in Table S1. Two separate transects of $\delta^{13}C_c$ measurements across the direction of shell growth were performed in two fragments of the same shell, mounted separately in epoxy. Closed symbols indicate measurements made with an 8 µm spot size; open symbols are from 6 µm diameter spot measurements (spatial resolution shown with horizontal error bars in box). See caption for Fig. 4 for detailed figure explanation.

SV-51 was either centered on the labeled calcite band and incorporated a fraction of ambient calcite on either side of the band, or was offset to one edge of the band with the ambient calcite beam overlap on the opposite side of the labeled band (Fig. 7b). We calculate that the width of the obliquely-cut band is between 6.3 and 6.6 µm, respectively, thereby confirming that a 6 µm spot could capture the full isotopic label in the chamber wall.

The range of measured ambient $\delta^{13}C_c$ values (excluding spot measurements in the analytical mixing zone) is slightly higher than the average predicted value of +2.5‰ VPDB from past culture experiments with *O. universa* grown under "high-light" conditions (Spero and Williams, 1988; Bemis et al., 2000; Table 3, Table S1; Figs. 4–6). At 19 and 22 °C, Bemis et al. (2000) reported individual shell values that ranged between 2.4‰ and 3.5‰. This range was likely due to differences between specimens in the impact of symbiont photosynthesis on shell $\delta^{13}C$, which is a result of symbiont density and perhaps the number of days of shell thickening before gametogenesis. Similar results have been observed from single-shell analyses of fossil *O. universa* from western equatorial Atlantic cores, where values >4‰ were measured in some individuals (Billups and Spero, 1996). Thus, it is unlikely that the ambient $\delta^{13}C_c$

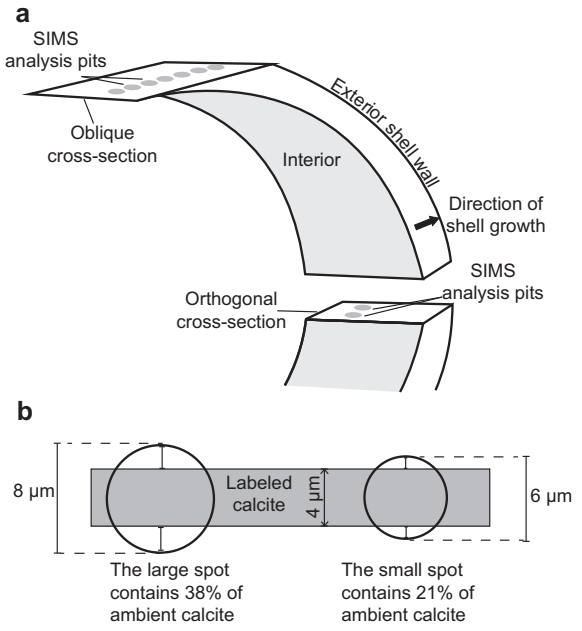

Fig. 7. (a) Schematic of a fragment of a spherical *O. universa* shell showing both orthogonal and oblique cross-sections. The oblique cross-section is able to accommodate more SIMS analysis pits (~1 µm deep) in the direction of growth, increasing the spatial resolution that can be achieved with multiple measurements. (b) Calculation of the width of a labeled band, based on an 8 or 6 µm spot with intermediate $\delta^{13}C_c$ that overlaps regions of both labeled and unlabeled calcite.

values we present here, which are higher than the Bemis et al. (2000) averages, are a result of our labeling experiment. Rather, we are probably observing normal inter-individual variation in shell geochemistry.

Spot $\delta^{13}C$ analyses in targeted domains of fossil foraminifer shells have the potential to address a suite of paleoceanographic questions not previously accessible using conventional IRMS techniques for carbon isotope analysis. For instance, Lohmann (1995) used a modeling approach and proposed that $\delta^{13}C$ variability among planktic foraminifer shells in a fossil assemblage could be due to a mixture of ontogenetic calcite, biogenic crust, and/or abiogenic calcite overgrowths that were added in different environments between the surface and bottom waters. Spot $\delta^{13}C_c$ analyses using SIMS across different sections of fossil foraminifers could resolve these sources if the surface-to-deep $\delta^{13}C_{DIC}$ gradient was sufficiently large to exceed the analytical uncertainty of individual measurements. Similarly, the SIMS technique may be able to resolve authigenic calcite addition in foraminifers influenced by oxidation of methane or other hydrocarbons in deep-sea sediment habitats (Hill et al., 2003; Torres et al., 2010; Panieri et al., 2012). In oceanic regions with large $\delta^{13}C_{DIC}$ gradients, such as the eastern equatorial Pacific thermocline ($\delta^{13}C_{DIC}$ gradient = ~2‰; Koutavas and Lynch-Stieglitz, 2003; Spero et al., 2003), SIMS analyses could provide a source of information for reconstructing the migration of individual specimens through the thermocline (Fairbanks et al., 1980, 1982). In species that do not migrate vertically, individual shell chemistry could record short-term spatial changes in $\delta^{13}C_{DIC}$, such as estuarine carbon isotope and salinity gradients (Kemp et al., 2010; Osterman and Smith, 2012). If such analyses were combined with SIMS $\delta^{18}O_c$ spot measurements (Kozdon et al., 2009, 2011, 2013; Vetter et al., 2013a), in theory one could reconstruct both temperature and nutrient/carbon isotope gradients from groups of individual fossil shells. Ultimately, SIMS $\delta^{13}C$ applications may be most valuable in exploring carbon isotope gradients during large planetary carbon cycle perturbations, such as the Paleocene-Eocene Thermal Maximum (PETM). Here, SIMS may offer a means to extract $\delta^{13}C$ data from unaltered regions of fossil shells, similar to the approach utilized by Kozdon et al. (2011) using SIMS-based $\delta^{18}O$ measurements.

4.2. Linking $\delta^{13}C$ with intrashell trace element data

Previous LA-ICP-MS trace element depth profiles on cultured *O. universa* demonstrate that instantaneous changes in seawater cation chemistry are resolvable within 1–2 µm with LA-ICP-MS depth profiling (Vetter et al., 2013a), and within <1 µm using nanoSIMS (Gagnon, pers. comm.). The Ba/Ca and $^{87}Sr/Ca$ depth profiles from cultured *O. universa* we present here exhibit spatial transitions over 4–10 s (Ba/Ca) and 2–8 s ($^{87}Sr/Ca$) of ablation time (Figs. 4a, d, 5a, 6a). These trace element depth profiles thus allow us to identify the position within shell calcite of the transfer into ^{13}C-labeled seawater, marked by the start of the rise in a trace element ratio (Ba/Ca). We cannot quantify the exact depth (µm) ablated in the shell because we have not calibrated our LA-ICP-MS system to convert ablation energy and number of laser pulses into ablated depth for a given laser energy. However, in pits with aspect ratio <2, the ablation rate is linear (Eggins et al., 1998; Woodhead et al., 2004). Since both LA-ICP-MS depth profiles and oblique shell cross-sections are linear, and both sets of measurements begin and end at the shell walls, we can evaluate trace element and SIMS data together (Figs. 4–6).

Previous experiments with live *O. universa* indicate that an intracellular inorganic carbon pool in this species is insignificant, if present at all (Bijma et al., 1999). Our LA-ICP-MS depth profiles measure intrashell Ba/Ca and $^{87}Sr/Ca$ that record nearly instantaneous changes in water chemistry. From these data, we hypothesize that $\delta^{13}C$ labels are likely recorded in shell calcite at the same time as elemental tracers, with little temporal lag due to a carbon pool. This supports previous results suggesting that simultaneous Ba and ^{18}O tracers are precipitated in shell calcite such that the analytical mixing zone of both SIMS and LA-ICP-MS is unable to resolve offsets between the two tracers (Vetter et al., 2013a). Intrashell trace element geochemistry on fossil foraminifers has been resolved within 2 µm using EPMA (Pena et al., 2005; Hathorne et al., 2009) or LA-ICP-MS (Pena et al., 2008; Sadekov et al., 2010; Bolton et al., 2011), which corresponds to calcification times of hours to days. Spatial patterns of trace element heterogeneity obtained from LA-ICP-MS depth profiles could therefore be used as a screening tool to target

potential intrashell domains of interest for spot isotopic analyses ($\delta^{13}C$, $\delta^{18}O$) using SIMS, which requires more intensive sample preparation and cost. Together, paired analyses of intrashell geochemical heterogeneity enable researchers to address questions about biological and ecological controls on shell geochemistry (Rollion-Bard and Erez, 2010; Bolton et al., 2011) and open the possibility of resolving a daily-scale record of changes in ocean chemistry from fossil foraminifer shells, within the limitations of the precision achievable in our study.

5. SUMMARY

In this study, we demonstrate that 6–7 μm thick bands with distinct $\delta^{13}C$ values in the shell walls of the planktic foraminifer *O. universa* can be resolved using *in situ* $\delta^{13}C$ analyses with SIMS. Mounting specimens in oblique polished cross-sections can increase the effective spatial resolution of these measurements. Analyses with a 6 μm diameter × 1 μm deep spot placed entirely within bands of ambient or ^{13}C-labeled calcite yield $\delta^{13}C$ values consistent with predicted values based on measured $\delta^{13}C_{DIC}$ and empirical, temperature-dependent calibrations. SIMS analyses using an 8 μm spot yield intermediate $\delta^{13}C$ values, and are unable to fully resolve isotopically-labeled bands, demonstrating the analytical mixing that occurs when a single spot measurement overlaps regions of shell calcite with different $\delta^{13}C$ values. This analytical mixing occurs across multiple bands of shell calcite with different geochemical compositions during both SIMS and LA-ICP-MS analyses. Cation (Ba and ^{87}Sr) and stable isotope (^{13}C and ^{18}O) tracers, measured linearly in the direction of shell growth, appear to be cross-correlated within the spatial resolution of the two analytical techniques. Experimental results here support the application of intrashell $\delta^{13}C$ measurements in foraminiferal calcite to paleoceanographic questions, if the $\delta^{13}C_{DIC}$ gradient is sufficient with respect to analytical precision.

ACKNOWLEDGEMENTS

We gratefully acknowledge the field assistance of A. Russell, J. Fehrenbacher, A. Gagnon, J. Snyder, K. Holland, and B. Wagman; and the staff of the Wrigley Marine Science Center on Catalina Island. We also thank N. Kita and J. Kern at WiscSIMS for analytical support, and D.C. Kelly provided assistance with sample preparation and logistics. This work benefited greatly from the careful and experienced sample preparation of B. Hess, and we thank him for his efforts on Superbowl Sunday. Collection equipment for culturing experiments was partially funded by the UC Davis Durrell Fund for graduate research. This research was supported by NSF awards OCE-0550703, OCE1061676, and EAR-0946297 (H.J.S.), and Los Alamos National Laboratory award IGPP:09-RFP-008 (C.I.M. and H.J.S.). WiscSIMS is partially supported by NSF-EAR (0319230, 1053466).

APPENDIX A. SUPPLEMENTARY DATA

Supplementary data associated with this article can be found, in the online version, at http://dx.doi.org/10.1016/j.gca.2014.04.049.

REFERENCES

Allison N. and Finch A. A. (2010) The potential origins and palaeoenvironmental implications of high temporal resolution $\delta^{18}O$ heterogeneity in coral skeletons. *Geochim. Cosmochim. Acta* **74**, 5537–5548. http://dx.doi.org/10.1016/j.gca.2010.06.032.

Bemis B. E., Spero H. J., Bijma J. and Lea D. W. (1998) Reevaluation of the oxygen isotopic composition of planktonic foraminifera: experimental results and revised paleotemperature equations. *Paleoceanography* **13**, 150–160.

Bemis B. E., Spero H. J., Lea D. W. and Bijma J. (2000) Temperature influence on the carbon isotopic composition of Globigerina bulloides and *Orbulina universa* (planktonic foraminifera). *Mar. Micropaleontol.* **38**, 213–228.

Bernat M., Church T. and Allegre C. J. (1972) Barium and strontium concentrations in Pacific and Mediterranean seawater profiles by direct isotope dilution mass spectrometry. *Earth Planet. Sci. Lett.* **16**, 75–80.

Bijma J., Spero H. J. and Lea D. W. (1999) Reassessing foraminiferal stable isotope geochemistry: impact of the oceanic carbonate system (experimental results). In *Use of Proxies in Paleoceanography: Examples from the South Atlantic* (eds. G. Fischer and G. Wefer). Springer-Verlag, Berlin Heidelberg, pp. 489–512.

Billups K. and Spero H. J. (1996) Reconstructing the stable isotope geochemistry and paleotemperatures of the equatorial Atlantic during the last 150,000 years: results from individual foraminifera. *Paleoceanography* **11**, 217–238.

Billups K., Channell J. E. T. and Zachos J. (2002) Late Oligocene to early Miocene geochronology and paleoceanography from the subantarctic South Atlantic. *Paleoceanography* **17**. http://dx.doi.org/10.1029/2000pa000568.

Bolton A., Baker J. A., Dunbar G. B., Carter L., Smith E. G. C. and Neil H. L. (2011) Environmental versus biological controls on Mg/Ca variability in *Globigerinoides ruber* (white) from core top and plankton tow samples in the southwest Pacific Ocean. *Paleoceanography* **26**, PA2219. http://dx.doi.org/10.1029/2010PA001924.

Boyle E. A. and Keigwin L. D. (1985) Comparison of Atlantic and Pacific paleochemical records for the last 215,000 years: changes in deep ocean circulation and chemical inventories. *Earth Planet. Sci. Lett.* **76**, 135–150. http://dx.doi.org/10.1016/0012-821x(85)90154-2.

CDIAC, 2014. http://cdiac.ornl.gov/trends/co2/iso-sio/graphics/iso-graphics.html.

Eggins S. M., Kinsley L. P. J. and Shelley J. M. G. (1998) Deposition and element fractionation processes during atmospheric pressure laser sampling for analysis by ICP-MS. *Appl. Surf. Sci.* **127–129**, 278–286. http://dx.doi.org/10.1016/S0169-4332(97)00643-0.

Eggins S., De Deckker P. and Marshall J. (2003) Mg/Ca variation in planktonic foraminifera tests: implications for reconstructing palaeo-seawater temperature and habitat migration. *Earth Planet. Sci. Lett.* **212**, 291–306. http://dx.doi.org/10.1016/s0012-821x(03)00283-8.

Eggins S. M., Sadekov A. and De Deckker P. (2004) Modulation and daily banding of Mg/Ca in *Orbulina universa* tests by symbiont photosynthesis and respiration: a complication for seawater thermometry? *Earth Planet. Sci. Lett.* **225**, 411–419. http://dx.doi.org/10.1016/j.epsl.2004.06.019.

Fairbanks R. G., Wiebe P. H. and Bé A. W. H. (1980) Vertical distribution and isotopic composition of living planktonic foraminifera in the western North Atlantic. *Science* **207**, 61–63.

Fairbanks R. G., Sverdlove M., Free R., Wiebe P. H. and Bé A. W. H. (1982) Vertical distribution and isotopic fractionation of

living planktonic foraminifera from the Panama Basin. *Nature* **298**, 841–844.

Hanson N. N., Wurster C. M., Eimf and Todd C. D. (2010) Comparison of secondary ion mass spectrometry and micro-milling/continuous flow isotope ratio mass spectrometry techniques used to acquire intra-otolith $\delta^{18}O$ values of wild Atlantic salmon (Salmo salar). *Rapid Commun. Mass Spectrom.* **24**, 2491–2498. http://dx.doi.org/10.1002/rcm.4646.

Hathorne E. C., James R. H. and Lampitt R. S. (2009) Environmental versus biomineralization controls on the intratest variation in the trace element composition of the planktonic foraminifera *G. inflata* and *G. scitula*. *Paleoceanography* **24**, PA4204. http://dx.doi.org/10.1029/2009pa001742.

Hill T. M., Kennett J. P. and Spero H. J. (2003) Foraminifera as indicators of methane-rich environments: a study of modern methane seeps in Santa Barbara Channel, California. *Mar. Micropaleontol.* **49**, 123–138. http://dx.doi.org/10.1016/s0377-8398(03)00032-x.

Hönisch B., Allen K. A., Russell A. D., Eggins S. M., Bijma J., Spero H. J., Lea D. W. and Yu J. (2011) Planktic foraminifers as recorders of seawater Ba/Ca. *Mar. Micropaleontol.* **79**, 52–57. http://dx.doi.org/10.1016/j.marmicro.2011.01.003.

Jonkers L., de Nooijer L. J., Reichart G. J., Zahn R. and Brummer G. J. A. (2012) Encrustation and trace element composition of *Neogloboquadrina dutertrei* assessed from single chamber analyses – implications for paleotemperature estimates. *Biogeosciences* **9**, 4851–4860. http://dx.doi.org/10.5194/bg-9-4851-2012.

Kemp A. C., Vane C. H., Horton B. P. and Culver S. J. (2010) Stable carbon isotopes as potential sea-level indicators in salt marshes, North Carolina, USA. *Holocene* **20**, 623–636. http://dx.doi.org/10.1177/0959683609354302.

Killingley J. S., Johnson R. F. and Berger W. H. (1981) Oxygen and carbon isotopes of individual shells of planktonic foraminifera from Ontong Java Plateau, Equatorial Pacific. *Palaeogeogr. Palaeoclimatol. Palaeoecol.* **33**, 193–204. http://dx.doi.org/10.1016/0031-0182(81)90038-9.

Koutavas A. and Lynch-Stieglitz J. (2003) Glacial-interglacial dynamics of the eastern equatorial Pacific cold tongue Intertropical Convergence Zone system reconstructed from oxygen isotope records. *Paleoceanography* **18**. http://dx.doi.org/10.1029/2003pa000894.

Kozdon R., Ushikubo T., Kita N. T., Spicuzza M. and Valley J. W. (2009) Intratest oxygen isotope variability in the planktonic foraminifer *N. pachyderma*: real vs. apparent vital effects by ion microprobe. *Chem. Geol.* **258**, 327–337. http://dx.doi.org/10.1016/j.chemgeo.2008.10.032.

Kozdon R., Kelly D. C., Kita N. T., Fournelle J. H. and Valley J. W. (2011) Planktonic foraminiferal oxygen isotope analysis by ion microprobe technique suggests warm tropical sea surface temperatures during the Early Paleogene. *Paleoceanography* **26**, PA3206. http://dx.doi.org/10.1029/2010pa002056.

Kozdon R., Kelly D. C., Kitajima K., Strickland A., Fournelle J. H. and Valley J. W. (2013) In situ $\delta^{18}O$ and Mg/Ca analyses of diagenetic and planktic foraminiferal calcite preserved in a deep-sea record of the Paleocene–Eocene thermal maximum. *Paleoceanography*. http://dx.doi.org/10.1002/palo.20048. 10.1002/palo.20048.

Lea D. W. and Spero H. J. (1994) Assessing the reliability of paleochemical tracers: barium uptake in the shells of planktonic foraminifera. *Paleoceanography* **9**, 445–452. http://dx.doi.org/10.1029/94PA00151.

Lea D. W., Martin P. A., Chan D. A. and Spero H. J. (1995) Calcium uptake and calcification rate in the planktonic foraminifer *Orbulina universa*. *J. Foramin. Res.* **25**, 14–23. http://dx.doi.org/10.2113/gsjfr.25.1.14.

Lohmann G. P. (1995) A model for variation in the chemistry of planktonic foraminifera due to secondary calcification and selective dissolution. *Paleoceanography* **10**. http://dx.doi.org/10.1029/95pa00059.

Mank A. J. G. and Mason P. R. D. (1999) A critical assessment of laser ablation ICP-MS as an analytical tool for depth analysis in silica-based glass samples. *J. Anal. Atom. Spectrom.* **14**, 1143–1153.

Marr J. P., Bostock H. C., Carter L., Bolton A. and Smith E. (2013) Differential effects of cleaning procedures on the trace element chemistry of planktonic foraminifera. *Chem. Geol.* **351**, 310–323. http://dx.doi.org/10.1016/j.chemgeo.2013.05.019.

Matta M. E., Orland I. J., Ushikubo T., Helser T. E., Black B. A. and Valley J. W. (2013) Ontogenetic migration of an eastern Bering Sea yellowfin sole *Limanda aspera* detected by otolith oxygen isotope analysis via ion microprobe. *Rapid Commun. Mass Spectrom.* **27**, 691–699.

Millo C., Sarnthein M., Erlenkeuser H., Grootes P. M. and Andersen N. (2005) Methane-induced early diagenesis of foraminiferal tests in the Southwestern Greenland Sea. *Mar. Micropaleontol.* **58**, 1–12. http://dx.doi.org/10.1016/j.marmicro.2005.07.003.

Olson I. C., Kozdon R., Valley J. W. and Gilbert P. (2012) Mollusk shell nacre ultrastructure correlates with environmental temperature and pressure. *J. Am. Chem. Soc.* **134**, 7351–7358. http://dx.doi.org/10.1021/ja210808s.

Osterman L. E. and Smith C. G. (2012) Over 100 years of environmental change recorded by foraminifers and sediments in Mobile Bay, Alabama, Gulf of Mexico, USA. *Estuar. Coast. Shelf Sci.* **115**, 345–358. http://dx.doi.org/10.1016/j.ecss.2012.10.001.

Panieri G., Camerlenghi A., Cacho I., Cervera C. S., Canals M., Lafuerza S. and Herrera G. (2012) Tracing seafloor methane emissions with benthic foraminifera: Results from the Ana submarine landslide (Eivissa Channel, Western Mediterranean Sea). *Mar. Geol.* **291**, 97–112. http://dx.doi.org/10.1016/j.margeo.2011.11.005.

Pena L. D., Calvo E., Cacho I., Eggins S. and Pelejero C. (2005) Identification and removal of Mn–Mg-rich contaminant phases on foraminiferal tests: implications for Mg/Ca past temperature reconstructions. *Geochem. Geophys. Geosyst.* **6**, Q09P02. http://dx.doi.org/10.1029/2005GC000930.

Pena L. D., Cacho I., Calvo E., Pelejero C., Eggins S. and Sadekov A. (2008) Characterization of contaminant phases in foraminifera carbonates by electron microprobe mapping. *Geochem. Geophys. Geosyst.* **9**, Q07012. http://dx.doi.org/10.1029/2008GC002018.

Rollion-Bard C. and Erez J. (2010) Intra-shell boron isotope ratios in the symbiont-bearing benthic foraminiferan *Amphistegina lobifera*: implications for $\delta^{11}B$ vital effects and paleo-pH reconstructions. *Geochim. Cosmochim. Acta* **74**, 1530–1536. http://dx.doi.org/10.1016/j.gca.2009.11.017.

Rollion-Bard C., Blamart D., Cuif J. P. and Juillet-Leclerc A. (2003) Microanalysis of C and O isotopes of azooxanthellate and zooxanthellate corals by ion microprobe. *Coral Reefs* **22**, 405–415. http://dx.doi.org/10.1007/s00338-003-0347-9.

Rollion-Bard C., Mangin D. and Champenois M. (2007) Development and application of oxygen and carbon isotopic measurements of biogenic carbonates by ion microprobe. *Geostand. Geoanal. Res.* **31**, 39–50. http://dx.doi.org/10.1111/j.1751-908X.2007.00834.x.

Rollion-Bard C., Erez J. and Zilberman T. (2008) Intra-shell oxygen isotope ratios in the benthic foraminifera genus *Amphistegina* and the influence of seawater carbonate chemistry and temperature on this ratio. *Geochim. Cosmochim. Acta* **72**, 6006–6014.

Russell A. D., Hönisch B., Spero H. J. and Lea D. W. (2004) Effects of seawater carbonate ion concentration and temperature on shell U, Mg, and Sr in cultured planktonic foraminifera. *Geochim. Cosmochim. Acta* **68**, 4347–4361. http://dx.doi.org/10.1016/j.gca.2004.03.013.

Sadekov A. Y., Eggins S. M., Klinkhammer G. P. and Rosenthal Y. (2010) Effects of seafloor and laboratory dissolution on the Mg/Ca composition of *Globigerinoides sacculifer* and *Orbulina universa* tests – a laser ablation ICPMS microanalysis perspective. *Earth Planet. Sci. Lett.* **292**, 312–324. http://dx.doi.org/10.1016/j.epsl.2010.01.039.

Schiffelbein P. and Hills S. (1984) Direct assessment of stable isotope variability in planktonic foraminifera populations. *Palaeogeogr. Palaeoclimatol. Palaeoecol.* **48**, 197–213.

Shieh Y. T., You C. F., Shea K. S. and Horng C. S. (2002) Identification of diagenetic artifacts in foraminiferal shells using carbon and oxygen isotopes. *J. Asian Earth Sci.* **21**, 1–5. http://dx.doi.org/10.1016/s1367-9120(01)00083-9.

Slowey N. C. and Curry W. B. (1995) Glacial-interglacial differences in circulation and carbon cycling within the upper western north-Atlantic. *Paleoceanography* **10**, 715–732.

Spero H. J. (1988) Ultrastructural examination of chamber morphogenesis and biomineralization in the planktonic foraminifer *Orbulina universa*. *Mar. Biol.* **99**, 9–20. http://dx.doi.org/10.1007/BF00644972.

Spero H. J. (1992) Do planktic foraminifera accurately record shifts in the carbon isotopic composition of seawater $\sum CO_2$? *Mar. Micropaleontol.* **19**, 275–285. http://dx.doi.org/10.1016/0377-8398(92)90033-g.

Spero H. J. and Lea D. W. (2002) The cause of carbon isotope minimum events on glacial terminations. *Science* **296**, 522–525.

Spero H. J. and Parker S. L. (1985) Photosynthesis in the symbiotic planktonic foraminifer *Orbulina universa*, and its potential contribution to oceanic primary productivity. *J. Foramin. Res.* **15**, 273–281. http://dx.doi.org/10.2113/gsjfr.15.4.273.

Spero H. J. and Williams D. F. (1988) Extracting environmental information from planktonic foraminiferal $\delta^{13}C$ data. *Nature* **335**, 717–719.

Spero H. J., Lerche I. and Williams D. F. (1991) Opening the carbon isotope "vital effect" black box, 2, quantitative model for interpreting foraminiferal carbon isotope data. *Paleoceanography* **6**, 639–655. http://dx.doi.org/10.1029/91pa02022.

Spero H. J., Bijma J., Lea D. W. and Bemis B. E. (1997) Effect of seawater carbonate concentration on foraminiferal carbon and oxygen isotopes. *Nature* **390**, 497–500.

Spero H. J., Mielke K. M., Kalve E. M., Lea D. W. and Pak D. K. (2003) Multispecies approach to reconstructing eastern equatorial Pacific thermocline hydrography during the past 360 kyr. *Paleoceanography* **18**. http://dx.doi.org/10.1029/2002pa000814.

Torres M. E., Martin R. A., Klinkhammer G. P. and Nesbitt E. A. (2010) Post depositional alteration of foraminiferal shells in cold seep settings: new insights from flow-through time-resolved analyses of biogenic and inorganic seep carbonates. *Earth Planet. Sci. Lett.* **299**, 10–22. http://dx.doi.org/10.1016/j.epsl.2010.07.048.

Valley J. W. and Kita N. T. (2009) In situ oxygen isotope geochemistry by ion microprobe. In *Secondary Ion Mass Spectrometry in the Earth Sciences* (ed. M. Fayek). Mineralogical Association of Canada, (Vol. 41, pp. 16–63).

Vetter L., Kozdon R., Mora C. I., Eggins S. M., Valley J. W., Hönisch B. and Spero H. J. (2013a) Micron-scale intrashell oxygen isotope variation in cultured planktic foraminifers. *Geochim. Cosmochim. Acta* **107**, 267–278. http://dx.doi.org/10.1016/j.gca.2012.12.046.

Vetter L., Spero H. J., Russell A. D. and Fehrenbacher J. S. (2013b) LA-ICP-MS depth profiling perspective on cleaning protocols for elemental analyses in planktic foraminifers. *Geochem. Geophys. Geosys.* **14**, 2916–2931. http://dx.doi.org/10.1002/ggge.20163.

Williams D. F., Be A. W. H. and Fairbanks R. G. (1981) Seasonal stable isotopic variations in living planktonic foraminifera from Bermuda plankton tows. *Palaeogeogr. Palaeoclimatol. Palaeoecol.* **33**, 71–102.

Wilson R. G. (1995) SIMS quantification in Si, GaAs, and diamond – an update. *Int. J. Mass Spectrom. Ion Processes* **143**, 43–49.

Woodhead J., Hergt J., Shelley M., Eggins S. and Kemp R. (2004) Zircon Hf-isotope analysis with an excimer laser, depth profiling, ablation of complex geometries, and concomitant age estimation. *Chem. Geol.* **209**, 121–135. http://dx.doi.org/10.1016/j.chemgeo.2004.04.026.

Zachos J., Pagani M., Sloan L., Thomas E. and Billups K. (2001) Trends, rhythms, and aberrations in global climate 65 Ma to present. *Science* **292**, 686–693.

Zachos J. C., Röhl U., Schellenberg S. A., Sluijs A., Hodell D. A., Kelly D. C., Thomas E., Nicolo M., Raffi I., Lourens L. J., McCarren H. and Kroon D. (2005) Rapid acidification of the ocean during the Paleocene–Eocene thermal maximum. *Science* **308**, 1611–1615. http://dx.doi.org/10.1126/science.1109004.

Zhang J., Quay P. D. and Wilbur D. O. (1995) Carbon isotope fractionation during gas–water exchange and dissolution of CO_2. *Geochim. Cosmochim. Acta* **59**, 107–114.

Associate editor: Claire Rollion-Bard